Determination of horizontal geostatic stress in clay with self-bored pressuremeter

M. G. JEFFERIES
Gulf Canada Resources, Frontier Development Division, P.O. Box 130, Calgary, Alta., Canada T2P 2H7

Received June 17, 1987
Accepted March 31, 1988

The Gibson–Anderson theory for interpretation of pressuremeter data in clay is extended to include the unloading part of the test for the particular circumstances that prevail with a self-bored pressuremeter (SBP). Incorporation of the extended theory in a computer-aided modelling procedure allows horizontal geostatic stress to be unambiguously determined from SBP data by image matching irrespective of imperfections in the self-boring process. The procedure is illustrated by example on a previously reported test carried out in Beaufort Shelf clay.

Key words: clay, *in situ* tests, self-bored pressuremeter, K_0.

La théorie de Gibson–Anderson pour l'interprétation des données du pressiomètre dans l'argile a été développée afin d'inclure la partie déchargement de l'essai de pressiomètre auto-foreur (SBP). L'incorporation de ce nouveau développement dans une procédure de modélisation assistée par ordinateur permet de déterminer de façon non ambiguë la contrainte géostatique horizontale en partant des données du SBP et par appariement d'image indépendamment des imperfections du processus d'auto-forage. La procédure est illustrée au moyen de l'exemple d'un essai sur l'argile du Plateau de la Mer de Beaufort qui a été publié précédemment.

Mots clés : argile, essais *in situ*, pressiomètre auto-foreur, K_0.

[Traduit par la revue]

Can. Geotech. J. 25, 559–573 (1988)

Introduction

The self-bored pressuremeter (SBP) is an instrument that may be introduced into a soil deposit with minimal disturbance. Once introduced into the soil, the soil may be tested by expanding the pressuremeter. Both expansion pressure and associated radial strain are measured during this test phase. Several important data may be deduced from the results of such a test, in particular the horizontal geostatic stress.

The self-bored pressuremeter test is one of the few techniques available for measuring the horizontal geostatic stress in a soil. However, acceptance of data obtained with a pressuremeter is a long way from universal, usually because the data on σ_{ho} obtained with the SBP is significantly different from the expected value. Indeed, Mesri and Castro (1987) have recently advanced the opinion that is not possible to measure σ_{ho} with any *in situ* technique. While it appears that the usual expectation of value for σ_{ho} is erroneous (Jefferies *et al.* 1987), it is also true that the detractors of the SBP do have a case regarding the manner in which σ_{ho} is inferred.

Determination of σ_{ho} from SBP data may be carried out with a number of different methods. To date eight techniques (initial "lift-off"; Arnold 1981; Denby 1978; Lacasse *et al.* 1981; Law and Eden 1982; Marsland and Randolph 1977; Wroth 1980; Jefferies *et al.* 1985) have been proposed. Lacasse and Lunne (1982) have compared the application of most of these methods to two soft clay sites. However, all amount to inspection of the data for an inflection point or the like during the initial 1% or so of radial expansion. As the detractors of the SBP point out, this is a subjective estimate, not a measurement. The SBP will also, in general, introduce some disturbance of the soil adjacent to the pressuremeter, and even if this disturbance is small, it may be sufficient to cause considerable uncertainty in σ_{ho}. An alternative procedure to the published methods for determination of σ_{ho} in clays is obviously desirable.

There appears to be a tendency to assume that σ_{ho} must be obtained from the initial part of the expansion curve. This is an unnecessary restriction. An examination of the various theories for interpretation of pressuremeter tests in clay illustrates that σ_{ho} information is carried throughout the entire expansion phase. However, as the expansion curve is the product of both σ_{ho} and the clay strength (or other constitutive parameters), there are infinite combinations of σ_{ho} and strength that will produce the measured curve. But there is no need to treat pressuremeter tests as only an expansion problem. The instrument is depressurized once the expansion phase of the test has been completed and this depressurization or contraction phase also carries information on soil behaviour. If information in the unloading phase of the test is utilized together with the expansion curve, then constitutive parameters and σ_{ho} may both be unambiguously found (at least within the limitations of the constitutive model employed).

The interpretation of *in situ* tests presents an inverse boundary value problem. One approach to the solution of such problems is computer-aided modelling (CAM). This approach involves the selection of numerical values for the various parameters in a theory from which a predicted pressure versus expansion–contraction curve is calculated. The theoretical curve is then visually compared with test data, numerical values are adjusted, and the theoretical curve recalculated until an acceptable image match is achieved. The process is called CAM because such image matching requires considerable numerical calculations and is, therefore, carried out interactively on a computer. CAM has the particular advantage of testing a complete theory against all the data, so that the optimum parameters for the chosen constitutive characterization of the soil may be found. It is also easy to explore the consequences of testing effects such as disturbance.

This paper uses CAM to show that σ_{ho} in clay may be unambiguously found from the SBP using an extended version of the Gibson and Anderson (1961) theory. Further, it is shown that the value of σ_{ho} so determined is insensitive to both disturbance during self-boring and deficiencies in the elastic–plastic characterization of clay strength.

Printed in Canada / Imprimé au Canada

Restrictions on pressuremeter type and test procedures

The work presented here is only valid for self-bored pressuremeters. This restriction is imposed because of the need to utilize the curvature of the pressure–displacement relationship during initial instrument expansion for proper image matching. It also allows the simplest theoretical treatment. Actual testing used Cambridge-type instruments (Hughes 1973) with direct strain gauge sensing of radial displacement, and the theory developed applies to this type of equipment. Subsequent work may allow further modification of the proposed technique to the push-in-pressuremeter (Henderson *et al.* 1979) or full displacement pressuremeters (Hughes and Robertson 1985). The need to use initial curvature would appear to preclude the use of the proposed technique with pressuremeters inserted into previously drilled boreholes.

The image-matching procedure makes use of the computational and graphic capabilities present in the current generation of "engineering work stations." This requires that the SBP data itself be brought into digital form. While it is possible to subsequently digitize data not originally recorded in digital form, this is not an efficient method of interpreting SBP data. Further, sufficient resolution must exist to preserve the curvatures and inflection points in the test data; this resolution must be obtained at data rates that maintain the undrained conditions assumed in the theory. Together, these requirements strongly indicate direct electronic digital data acquisition during testing as a prerequisite to the interpretation methodology presented here. SBP data that have been processed to date were obtained in this manner (described in Hughes *et al.* 1984) and each test typically comprises about a thousand scans obtained at a scan rate of 1.5 Hz.

A closed-form solution for a complete SBP test in clay

Background

Interpretation of SBP tests using CAM requires a theoretical model for the test. Such a model can be either a closed-form or numerical solution to the expansion-collapse of a cylindrical cavity. A closed-form solution is considerably more convenient than a numerical one; an extension of the solution provided by Gibson and Anderson (1961) offers the simplest closed-form solution with which to explore the CAM technique to interpretation of SBP data. The required extension is developed below; a description of the principal features of a complete SBP test is given first.

Complete pressuremeter test

A complete self-bored pressuremeter test involves at least four activities: (i) insertion by self-boring; (ii) expansion of the instrument; (iii) unload–reload loop(s); (iv) contraction of the instrument.

Commonly, all activities are carried out but no data are recorded during the fourth stage. Indeed, contraction is usually only undertaken for the purpose of removal or advancement of the instrument. The interpretation procedure presented here requires that this fourth (contraction) stage be regarded as equally important to the initial expansion and that detailed data acquisition be continued until the instrument is completely depressurized.

The insertion is carried out, minimizing disturbance to the adjacent soil, so that the instrument becomes located vertically in the clay, with the stresses existing in the clay being those prevailing prior to insertion. The situation is summarized as stage 0 in Fig. 1.

The pressuremeter is then expanded. Expansion is carried out rapidly so that undrained conditions occur. Initially, the clay behaves elastically as the pressure in the instrument increases, which produces the situation illustrated as stage 1 in Fig. 1. The pressure is then further increased until the shear stress in the clay equals the yield strength. At this pressure the test moves into stage 2, where a progressively larger annulus of plastic material surrounds the SBP as the pressuremeter is expanded. The far field remains elastic, however, and the stress field is illustrated in stage 2 of Fig. 1. Eventually, expansion of the pressuremeter is terminated.

The pressure in the SBP is then reduced and unloading commences. Unloading is also carried out rapidly, preserving undrained conditions. The reduction in stress at the pressuremeter itself is immediately transmitted in an elastic manner to the far field. This immediate transition to elastic behaviour occurs because the change in stress at the start of unloading causes the principal stress difference $\sigma_r - \sigma_\theta$ to fall below the yield condition throughout the domain. The new stress field may be conveniently thought of as the stress conditions prevailing in stage 1 being subtracted in ever increasing amounts from the residual stresses existing at the end of the expansion phase. An example of the situation prevailing during the initial part of the unloading cycle is shown as stage 3 in Fig. 1.

Continuation of unloading eventually leads to the situation where σ_θ becomes the major principal stress and σ_r the minor. Further unloading eventually produces yield of the clay. Again, yield is initiated at the SBP and extends outward as an ever increasing annular ring. The stress situation is now somewhat more complex and is shown as stage 4 in Fig. 1. Unloading continues in this manner until the pressuremeter returns to its original radius.

Assumptions

All existing analyses of pressuremeter tests contain assumptions and many are required for the analysis presented here. The necessary assumptions are conventionally accepted and are listed below:

(i) The analysis is restricted to undrained conditions prevailing throughout the test from the start of expansion to the completion of the contraction.

(ii) Test may be treated as expansion of a cylindrical cavity in a infinite medium (i.e., radially symmetric plane strain).

(iii) The vertical stress is and remains the intermediate principal stress.

(iv) The constitutive behaviour of the clay is simply elastic – perfectly plastic.

(v) The plastic strength of the clay may be represented by a simple Tresca criterion (i.e., S_u is unique).

(vi) The ratio of the unloading strength of the clay to the loading strength is known. For simplicity they will be taken as equal in development of the extended theory.

It should be noted that the analysis is carried out using "total" stresses.

The characterization of clay behaviour as elastic – Tresca-plastic is commonly made during the interpretation of *in situ* tests in clay and appears to be generally regarded as adequate (Wroth 1984).

Theoretical considerations

The assumptions listed above provide the simplest possible representation of a complete pressuremeter test. Further, these assumptions are identical to those made by Gibson and Anderson (1961), so that stages 1 and 2 of the complete test may

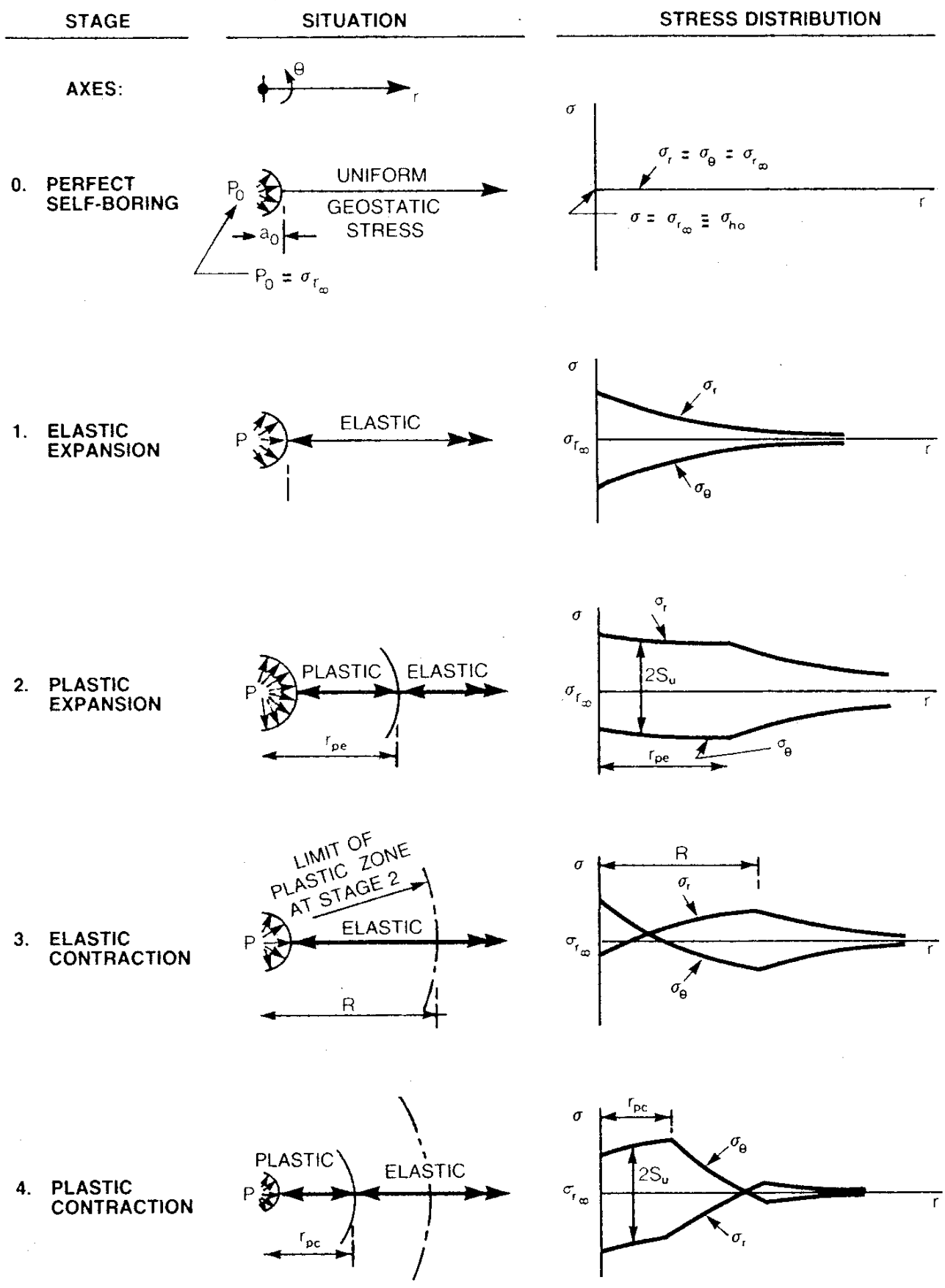

FIG. 1. Illustration of the five stages in a complete SBP test in clay.

directly use the equations developed by those authors provided due allowance is made for the change to self-bored rather than predrilled (Menard) testing. Specifically, the following equations apply.

Stage 1

$$[1a] \quad \sigma_r = \sigma_{ho} + (p - \sigma_{ho})\left(\frac{a_0}{r}\right)^2$$

$$[1b] \quad \sigma_\theta = \sigma_{ho} - (p - \sigma_{ho})\left(\frac{a_0}{r}\right)^2$$

$$[2] \quad \frac{a - a_0}{a_0} = \frac{(p - \sigma_{ho})}{2G}$$

Stage 1 terminates when yield first occurs. The yield criterion is

$$[3] \quad \sigma_r - \sigma_\theta = 2S_u$$

Substituting [1*a*] and [1*b*] in [3] provides the condition for the limit of stage 1:

$$[4] \quad P_{1L} = \sigma + S_u$$

with yield occurring first at the wall of the borehole in contact with the SBP, and P_{1L} being the corresponding pressure exerted by the SBP.

Stage 2

When the pressure in the SBP is increased beyond P_{1L} then stage 2 of the test is entered. During this phase the stress distributions are

$$[5a] \quad \sigma_r = p - 2S_u \ln\left(\frac{r}{a}\right), \qquad a < r < r_{pe}$$

$$[5b] \quad \sigma_r = \sigma_{ho} - S_u\left(\frac{r_{pe}}{r}\right)^2, \qquad r_{pe} < r < \infty$$

$$[5c] \quad \sigma_\theta = \sigma_r - 2S_u, \qquad a < r < r_{pe}$$

$$[5d] \quad \sigma_\theta = \sigma_{ho} - S_u\left(\frac{r_{pe}}{r}\right)^2, \qquad r_{pe} < r < \infty$$

where r_{pe} is the radius of the elastic–plastic transition; the relationship between pressure and outside diameter of the SBP is given by

$$[6] \quad p = \sigma_{ho} + S_u + S_u \ln\left[\frac{G}{S_u}\left(1 - \left(\frac{a_0}{a}\right)^2\right)\right]$$

Equations [1]–[6] provide information both necessary and sufficient to describe the expansion phase of a pressuremeter test. It should be noted that the equations describe the p versus a relationship in terms of just three parameters: G, S_u, σ_{ho}. An equivalent expression to [6] has been previously reported for the SBP by Windle and Wroth (1977).

Stage 3

Equations [5*a*]–[5*d*] describe the stress field during the expansion phase of the SBP test when plastic deformation of the clay is occurring. These equations apply from initiation of plastic yielding until expansion of the SBP is terminated. In particular, at the termination of expansion the stress distribution will be given by

$$[7a] \quad \sigma_r|_{max} = P_{max} - 2S_u \ln\left(\frac{r}{a_{max}}\right), \qquad a_{max} < r < R$$

$$[7b] \quad \sigma_r|_{max} = \sigma_{ho} + S_u\left(\frac{R}{r}\right)^2, \qquad R < r < \infty$$

$$[7c] \quad \sigma_\theta|_{max} = \sigma_r|_{max} - 2S_u, \qquad a_{max} < r < R$$

$$[7d] \quad \sigma_\theta|_{max} = \sigma_{ho} - S_u\left(\frac{R}{r}\right)^2, \qquad R < r < \infty$$

where P_{max} is the maximum expansion pressure applied to the SBP and a_{max} is the corresponding radius of the instrument at this pressure. This maximum expansion of the instrument caused the plastic–elastic transition in the clay to move outwards to a radius of R, which is also a maximum.

Contraction of the instrument follows the expansion phase. The unloading of the soil that accompanies the contraction occurs from the stress state described by [7*a*]–[7*d*]. Initially the unloading is elastic and the stress increments that arise as the pressure in the SBP is lowered are

$$[8a] \quad \Delta\sigma_r = (P - P_{max})\left(\frac{a_{max}}{r}\right)^2$$

$$[8b] \quad \Delta\sigma_\theta = -(p - p_{max})\left(\frac{a_{max}}{r}\right)^2$$

It should be noted that the "initial" cavity for the contraction phase is taken as a_{max}, the maximum cavity size. Further, $P < P_{max}$ so that $\Delta\sigma_r$ will be negative and $\Delta\sigma_\theta$ positive. The actual stress field during the third stage of the pressuremeter test is given by the simple addition of equations [7*a*]–[7*d*] and [8*a*]–[8*b*], since the prevailing elastic conditions allow superposition:

$$[9a] \quad \sigma_r = \sigma_r|_{max} + \Delta\sigma_r$$

$$[9b] \quad \sigma_\theta = \sigma_\theta|_{max} + \Delta\sigma_\theta$$

The relationship between the SBP pressure and radius of the instrument during this third stage may also be obtained in a similar manner. The elastic displacement induced by the change in SBP pressure is obtained in an analogous way to [2], giving

$$[10] \quad \frac{a - a_{max}}{a_{max}} = \frac{(p - p_{max})}{2G}$$

Now, in general, stage 3 cannot last forever, as at some (decreasing) pressure the ground will be insufficiently strong to support the stresses caused by the expanded borehole. Specifically, plastic strain in unloading will occur when

$$[11] \quad \sigma_\theta - \sigma_r = 2S_u$$

The situation may be understood by reference to Fig. 2. This figure illustrated the deviatoric stress state (Fig. 2*a*) prevailing at the end of stage 2 from which progressively increasing elastic deviatoric stress increments (Fig. 2*b*) are to be subtracted. Superposition of Figs. 2*a* and 2*b* shows clearly that yield will occur first at the SBP–ground interface, that is, when

$$[12] \quad r = a_{3L} = a_{max}\left(1 - \frac{S_u}{G}\right)$$

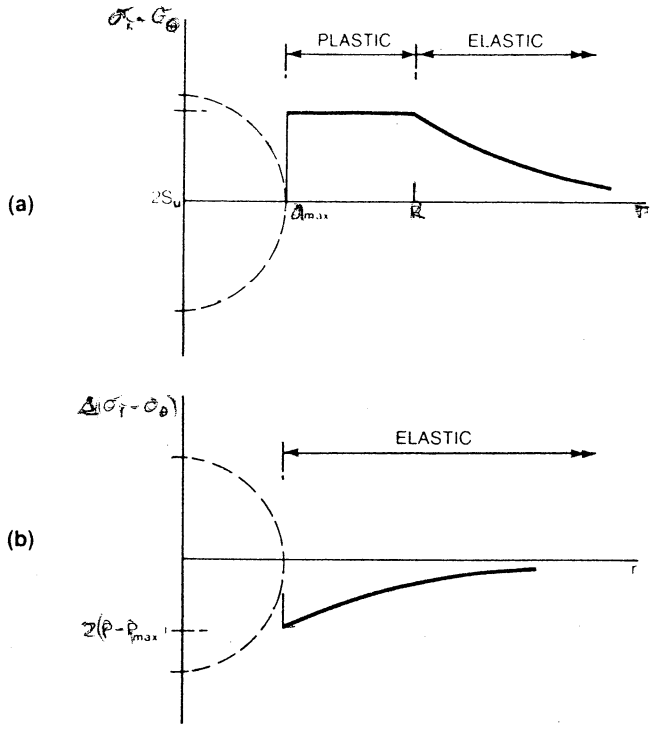

FIG. 2. Deviatoric stress distributions: (*a*) at peak load; (*b*) incremental during initial unloading.

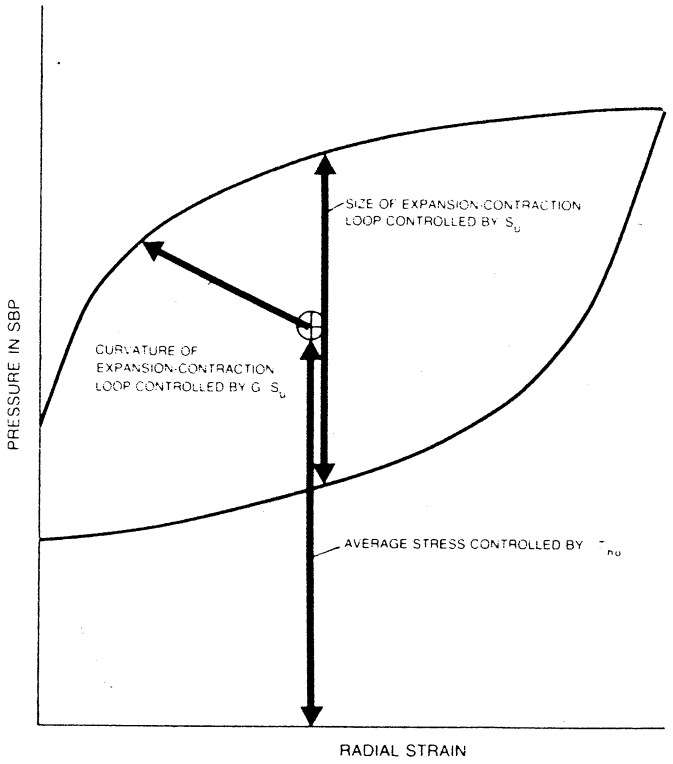

FIG. 3. Influence of variables in model of a complete SBP test.

The value of decreasing pressure at which this occurs may be found by substituting [9*a*] and [9*b*] in [11]:

$$[13] \quad \sigma_\theta - \sigma_r = \sigma_\theta|_{max} + \Delta\sigma_\theta - \sigma_r|_{max} - \Delta\sigma_r = 2S_u$$

which, upon substitution of [7*c*] into [13] and noting that $\Delta\sigma_\theta = -\Delta\sigma_r$, gives the intermediate result

$$[14] \quad \Delta\sigma_r = 2S_u, \qquad a_{max} < r < R$$

Notice that [14] is valid at the plastic–elastic interface during unloading regardless of the current radius (r_{pc}) of that interface provided that $r_{pc} < R$. This intermediate result will be used later. Further substitution of [8*a*] into [14] using [12] gives the criterion for the end of stage 3 in terms of SBP pressure, P_{3L}:

$$[15] \quad P_{3L} = P_{max} - 2S_u$$

It is worth noting that stage 3 is an elastic stage, which implies that only small unloading deformations occur until the internal pressure in the SBP has been lowered by approximately twice the strength of the clay. Equation [15] has been previously reported by Windle and Wroth (1977).

Stage 4

The final stage of the pressuremeter test—plastic cavity collapse—leads to a slightly more complex theory than the previous stages. Nevertheless, it is possible to develop the theory by extending the methodology used by Gibson and Anderson. First, the well-known equation of equilibrium for cylindrical coordinates

$$[16] \quad \frac{\partial\sigma_r}{\partial r} + \frac{\sigma_r - \sigma_\theta}{r} = 0$$

must hold throughout the domain. During stage 4 the pressure in the SBP is such that a plastic annulus extends from the outside of the SBP to a radius r_{pc}. In the zone $a < r < r_{pc}$, a state of plastic yielding exists in which

$$[17] \quad \sigma_\theta - \sigma_r = 2S_u$$

which upon substitution in [16] allows solution of the differential equation by separation of variables. Remembering that at the SBP $\sigma_r = P$ when $r = a$, it is found that

$$[18a] \quad \sigma_r = P + 2S_u \ln\left(\frac{r}{a}\right)$$

$$[18b] \quad \sigma_\theta = \sigma_r + 2S_u$$

Now at the interface between the plastic and elastic regions during the contraction, which is at a radius $r = r_{pc}$, the radial stress currently is from equation [18*a*]:

$$[19] \quad \sigma_r|_{r_{pc}} = P + 2S_u \ln\left(\frac{r_{pc}}{a}\right)$$

but at this same location the stress at the time of maximum internal pressure was from [7*a*]:

$$[20] \quad \sigma_r|_{max, r_{pc}} = P_{max} - 2S_u \ln\left(\frac{r_{pc}}{a_{max}}\right)$$

so that the radial stress change that has occurred in the soil at the current elastic–plastic interface is

$$[21] \quad \Delta\sigma_r|_{r_{pc}} = P - P_{max} - 2S_u \ln\left(\frac{r_{pc}^2}{a\, a_{max}}\right)$$

However, the interesting condition that the interface is just on the point of yielding means (after [14]) that

$$\Delta\sigma_r|_{r_{pc}} = -2S_u$$

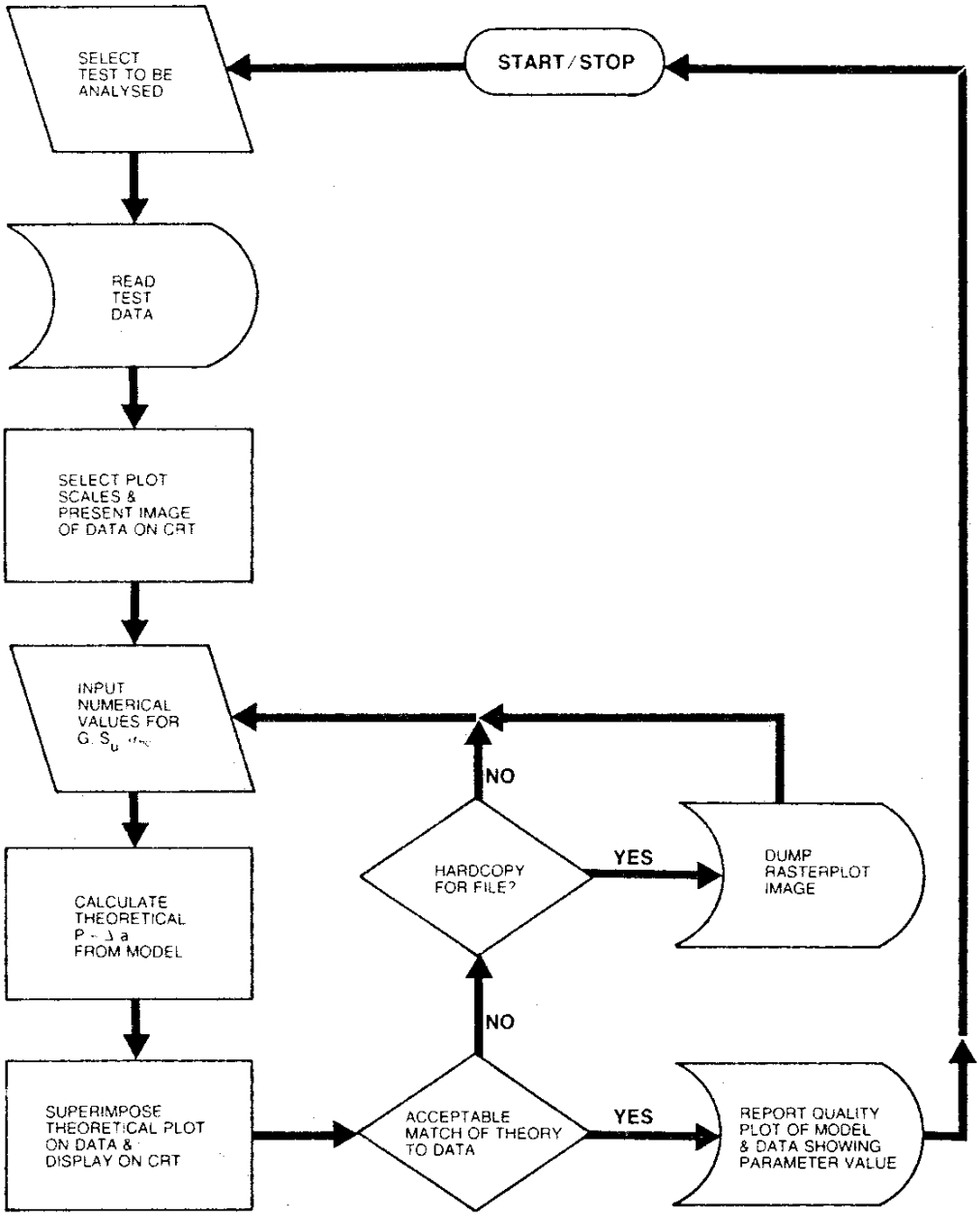

FIG. 4. Flow chart of computer-aided modelling (CAM) for interpretation of SBP data.

which may be used to eliminate $\Delta\sigma_r$ and provide the following relationship:

$$[22] \quad P = P_{max} - 2S_u - 2S_u \ln\left(\frac{r_{pc}^2}{a\, a_{max}}\right)$$

Turning now from stress conditions to displacements, the stress change at the elastic–plastic interface given by [21] will produce a corresponding elastic displacement of the interface (which will be negative and directed inward) of

$$[23] \quad u = \frac{\Delta\sigma_r|_{r_{pc}}}{2G} = -\frac{S_u\, r_{pc}}{G}$$

The condition that the clay remains undrained throughout the entire test is now utilized. The clay currently in the annulus $a < r < r_{pc}$ has a volume per unit height of $\pi(r_{pc}^2 - a^2)$ but also existed with the same volume in the annulus $a_{max} < r < (r_{pc} - u)$ at the end of expansion, and at this time the volume per unit height was $\pi[(r_{pc} - u)^2 - a_{max}^2]$. Since the two unit volumes are equal by the assumption of undrained loading it is found (neglecting second-order terms) that:

$$[24] \quad 2r_{pc}u = a^2 - a_{max}^2$$

and substituting [23] for u in [24] gives, after rearrangement,

$$[25] \quad \frac{r_{pc}^2}{a\, a_{max}} = \left(\frac{a_{max}}{a} - \frac{a}{a_{max}}\right)\left(\frac{G}{2S_u}\right)$$

Finally, the relationship between p and a during the fourth stage of the pressuremeter test may be found by substituting [25] in [22], to give

$$[26] \quad P = P_{max} - 2S_u - 2S_u \ln\left[\left(\frac{a_{max}}{a} - \frac{a}{a_{max}}\right)\left(\frac{G}{2S_u}\right)\right]$$

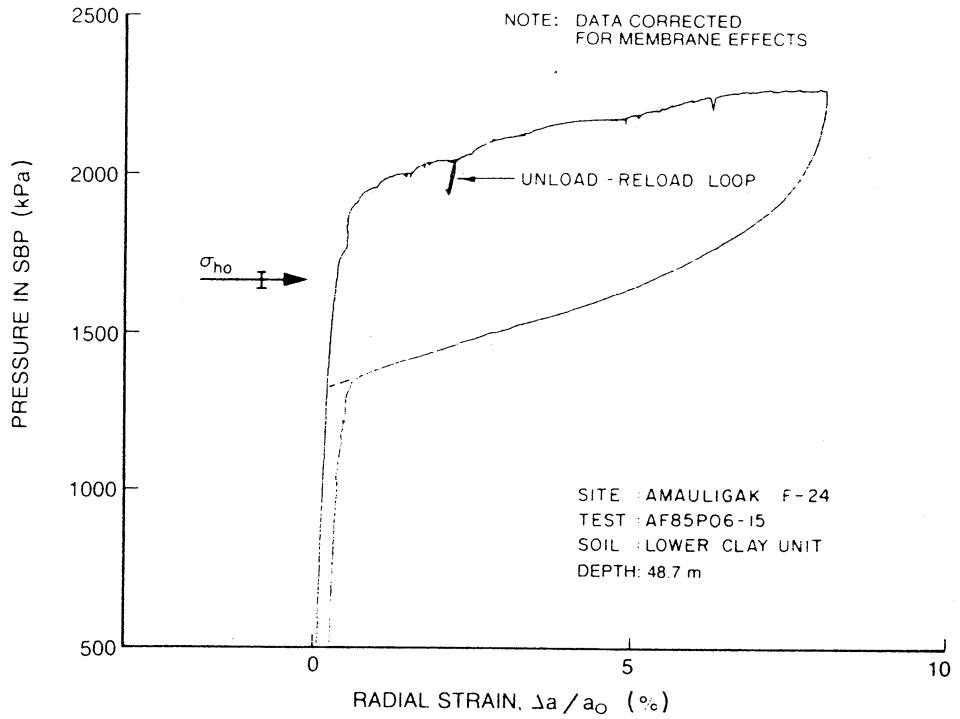

FIG. 5. Example of SBP data obtained at Amauligak F-24 site (after Jefferies *et al.* 1987).

The above equations provide a mathematical description of a complete SBP test in terms of an elastic–plastic soil model in undrained conditions.

Computer-aided modelling of the SBP test

Computer-aided modelling (CAM) allows numerical experimentation on a particular domain with particular properties, using a pertubation that characterizes the actual field experiment. The numerically computed experimental output is then compared with the actual experiment; parameters in the numerical experiment are then modified and the comparison repeated. Several such numerical experiments provide evidence for the values of the parameters sought, as well as providing direct information on how well conditioned the actual experiment is. This latter point is particularly important, as there may be several (if not many) solutions to the inverse problem and one is not necessarily to be preferred over another. It should also be appreciated that the numerical values of the various parameters are explicitly known at every step; if the image match is regarded as acceptable, then the values of the engineering parameters are defined without interpretation or judgment within the limits imposed by the inverse nature of the problem.

The interpretation of self-bored pressuremeter results in clay is a straightforward problem, provided the loading is applied rapidly (undrained). The solution for an elastic–Tresca-plastic model presented earlier involves just three variables (G, S_u, and σ_{ho}). The solution is also well conditioned for analysis of a complete pressuremeter test in that the three variables have quite distinct effects on the model, as illustrated in Fig. 3. The horizontal geostatic stress defines the average stress level of the model as well as the undisturbed "lift-off" pressure. The undrained strength largely controls the difference between limit pressure in expansion and the corresponding limit pressure in collapse. The shear modulus dominates the curvature of the pressure–displacement relationship during both the expansion and contraction stages of the test. This distinct separation of function of each variable allows reasonable fits of theory to data to be achieved in a few iterations, even by inexperienced persons. The flow chart for the modelling program used is presented in Fig. 4.

The number of iterations required to fit the theoretical curve to actual test data depends on the understanding and experience of the modeller. But the results are not dependent upon either factor provided due diligence is given to obtaining a fit. An experienced *in situ* testing engineer should have no difficulty in achieving acceptable model fits to data within five or six trials.

The "modelling" approach to SBP interpretation may readily be carried out using the current generation of microprocessor-based "engineering work stations." However, as the method involves visual comparison of graphical images, it is important to use a screen resolution of at least 600 × 400 pixels; modern CAD–CAM screens with 1024 × 1024 pixels are ideal. It is also helpful to utilize the latest generation of processors so that the modelling may be real-time interactive; the work described in this paper used a HP320 system.

Application of CAM to an SBP test

A considerable amount of SBP testing has been carried out in the Canadian Beaufort Shelf since 1980 and a summary of this work as it pertains to the horizontal geostatic stress in clay was recently presented in this journal (Jefferies *et al.* 1987). Since these data indicate unusually large (compared with the traditional expectation) horizontal stresses in the clays, it presents an excellent test for the new approach to SBP interpretation.

The previous paper (Jefferies *et al.* 1987) presented detailed data from a site known as Amauligak F-24, one such SBP Test being shown in Fig. 5. This test was carried out in a stiff clay approximately 48 m below mudline in 32 m of water (i.e., a total of 80 m below mean sea level), in a massive clay unit referred to as unit D1. The clay is a horizontally bedded silty

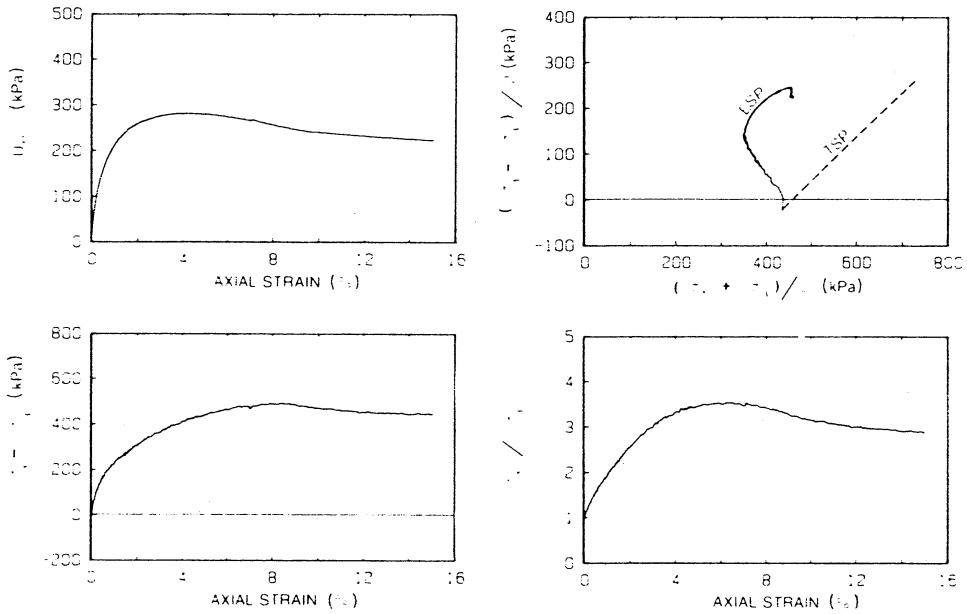

FIG. 6. Constitutive behaviour of stiff clay adjacent to SBP test AF85P06-15. (Anisotropically consolidated undrained strain-controlled triaxial test results; site: Amauligak F-24; borehole: AF85S06B; sample depth: 49.1 m.)

clay with I_P ranging from 15 to 25%; the water content is uniform with depth, actual values being in the narrow range of 28–32%; the corresponding liquidity index is close to zero throughout the unit.

The constitutive behaviour of this particular stiff clay is illustrated by some test data in Fig. 6, which shows the results of a triaxial test on a sample of the clay from approximately the same elevation as the SBP test. The sample was reconsolidated to the estimated *in situ* effective stress state (i.e., with K_0 = 1.1) before being sheared undrained. Figure 5 presents both stress–strain and stress path behaviour of the clay. The clay shows an initially contractive response to load and rapidly becomes dilatant after very limited strain, while the stress–strain curve shows marked work hardening to peak shear stress, which is followed by a very modest drop in strength with increased strain.

A basic assumption used in the derivation of the theory was isotropy of undrained strength. This issue has been examined by testing of Beaufort Sea clay with several stress paths (Jefferies *et al.* 1985), and it has been found that "extension" strengths in triaxial shear are comparable to the compression strengths. While this does not prove equality of strength after a principal stress rotation of 90°, it does suggest that equality is a reasonable first assumption. The issue will be addressed at greater length later.

The model of the complete SBP test was applied to the test data shown in Fig. 5 using G as a "free parameter." This allows optimization of the model to the expansion–contraction data unconstrained by the requirement to match the unload–reload loop (which defines the true shear modulus). The results of this modelling are shown in Fig. 7*a* and it can be seen that an excellent fit has been achieved between theory and data.

One point that should not be overlooked in using G as a free parameter is the need to also float a_{max}. If a value of G that is smaller than the unload–reload modulus is used in the model, then the model will poorly represent the initial unloading behaviour from a_{max}. An improved model is achieved by choosing a value for a_{max} in the model slightly greater than the actual one in the data, the choice being made so that the elastic strain recovered at midpoint of the elastic unloading is the same for the model as actual test data (Fig. 7*a*).

An advantage of CAM is that the numerical values of the various parameters are explicitly known at every stage. This is shown in Fig. 7*a* by the block in the lower right of the plot, which gives the values used to produce the particular model shown . If the fit of model to data is regarded as acceptable, then the parameter values are unarguable. This includes σ_{ho}, and it can be seen from Fig. 7*a* that σ_{ho} = 1690 kPa for this particular test. The previous work on this data (Jefferies *et al.* 1987) used a modified inspection technique to estimate σ_{ho} and reported 1670 ± 30 kPa for the same test, a slight understatement of the value determined by a complete model.

The modelling presented above has used G as a free parameter. Inspection of Fig. 7*a* shows that such an approach results in an initial loading–unloading stiffness that is much softer than the measured unload–reload loop (which is the true G for the clay). However, it is possible to match this unload–reload behaviour, as is illustrated in Fig. 7*b*. It is apparent from this latter figure that such matching produces a model of the expansion–contraction behaviour that is significantly different from the data, although a good fit is still achieved at the respective limit pressures. A comparison of the values for G shown in Figs. 7*a* and 7*b* shows that, whereas approximately 45 MPa corresponds to the unload–reload value, the best fit to the overall SBP data is obtained with 10 MPa. Examination of the constitutive test data (Fig. 6) shows that the first value corresponds to the initial tangent modulus, while the second value is marginally stiffer than the secant modulus at peak stress ratio. It would appear, therefore, that the model predictions are consistent with the triaxial test data. However, the inferred undrained strength is quite different. The SBP model indicates S_u = 155 kPa with the best-fit model, in contrast to an S_u > 220 kPa indicated by the triaxial test. Why there should be such a difference is not quite apparent.

Interestingly, the horizontal geostatic stress inferred from the test data remains sensibly constant ($\sigma_{ho} \approx$ 1700 kPa) during

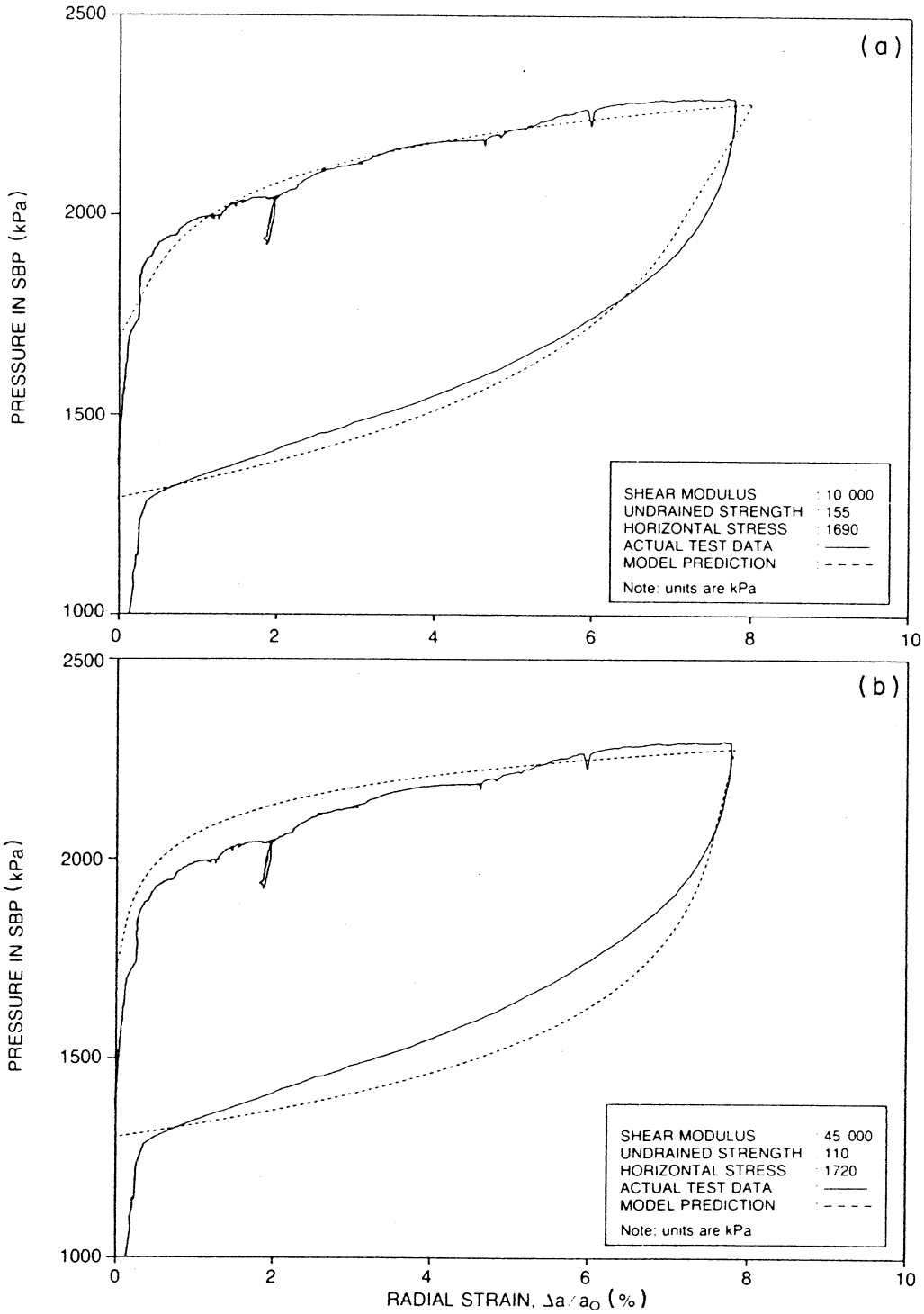

FIG. 7. Example of model fit to test data: (*a*) using G as a free parameter for best fit; (*b*) using G as determined by unload–reload loop. (Data from test AF85P06-15.)

these variations. This happens because the model is constrained to match both expansion and contraction limit pressures, and the average of these is strongly related to σ_{ho}. Thus, σ_{ho} is a well-conditioned measurement from an SBP test, as it is not strongly influenced by the choice of constitutive parameters.

Effect of strength anisotropy

One assumption made during the development of the closed-form solution was that the strength of the clay in loading was equal to that in unloading. One obvious consequence of this assumption is that strength anisotropy could lead to a questioning of the inferred—an undesirable—result.

The assumption of strength isotropy is not required in general. If the unloading strength of the clay during the SBP contraction phase, S_{u_c}, is taken to be a simple fraction (β) of the loading strength, then

$$S_{u_c} = \beta S_u \quad [27]$$

It is a straightforward matter to then go through [11]–[26]

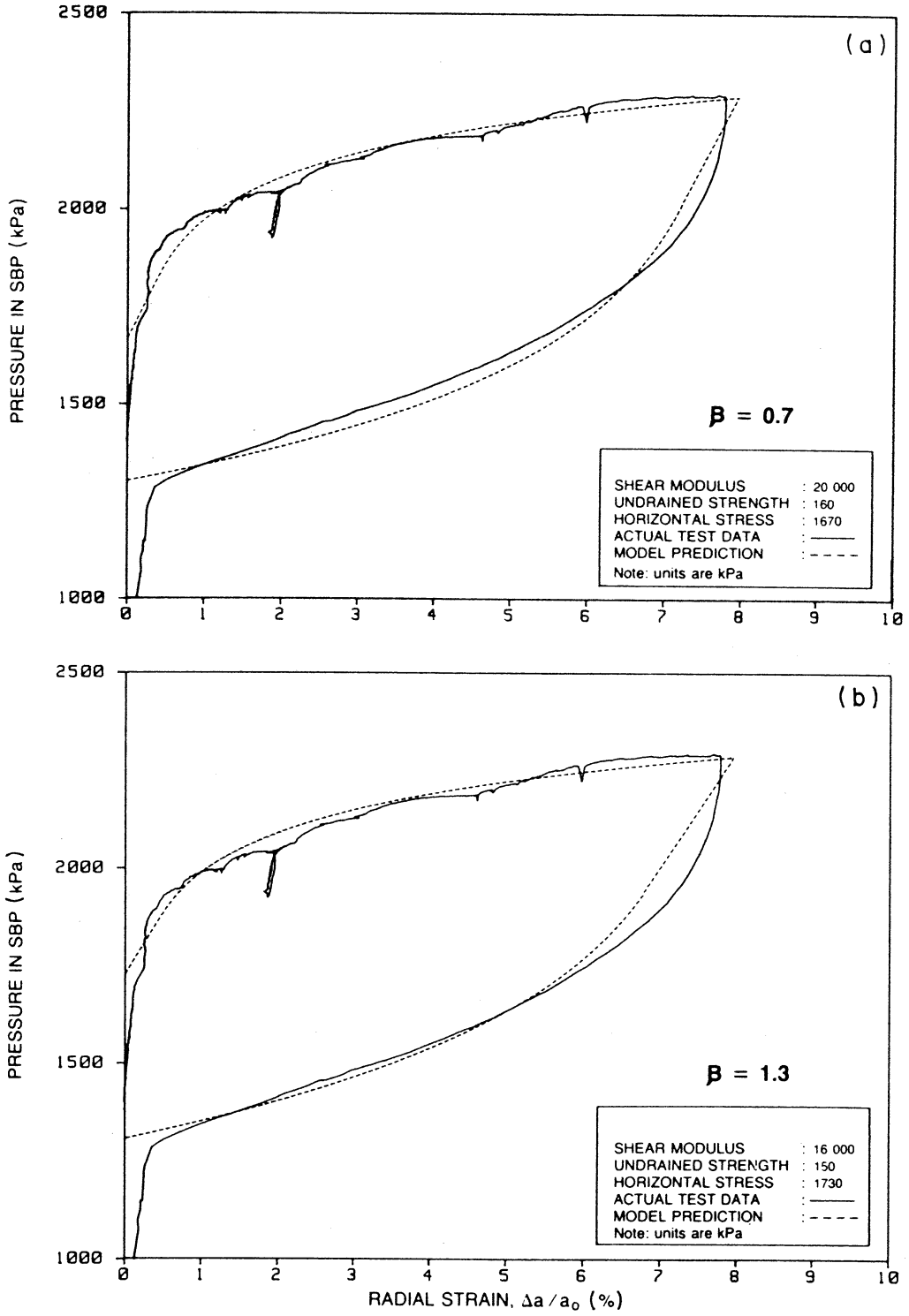

FIG. 8. Effect of strength anisotropy on interpretation of SBP data. (Data from test AF85P06-15.)

again, using [27] where appropriate, a process that leads to a slightly more complicated result equivalent to [15] and [26]. Specifically, it is found that

[28] $$P_{3L} = P_{max} - (1 + \beta)S_u$$

[29] $$P = P_{max} - (1 + \beta)S_u - S_u \ln\left\{\left[1 - \left(\frac{a}{a_{max}}\right)^2\right]\left[\frac{G}{(1 + \beta)^* S_u}\right]\right\}$$

$$- \beta S_u \ln\left\{\left[\left(\frac{a}{a_{max}}\right)^2 - 1\right]\left[\frac{G}{(1 + \beta)S_u}\right]\right\}$$

The consequence of using [28] and [29] as opposed to the assumption of strength isotropy is shown in Fig. 8 for two choices of β: 0.7 and 1.3.

The choice of $\beta = 0.7$ corresponds to a material that weakens during principal stress rotation by an arbitrary 30%. It can be seen from Fig. 8 that the consequence is that the com-

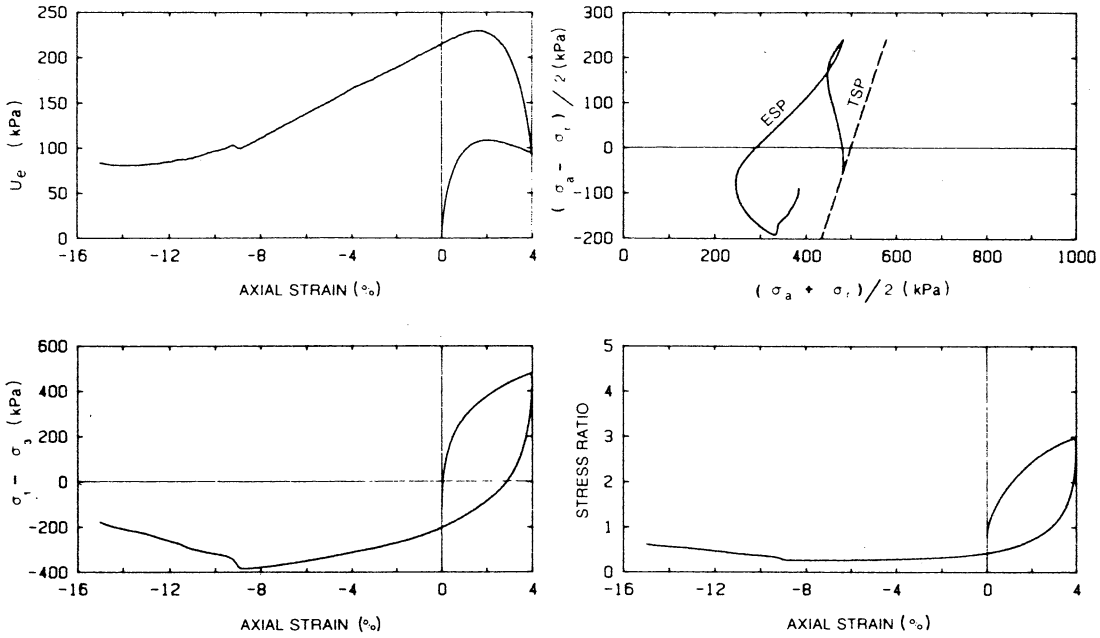

FIG. 9. Effect of shear stress reversal on clay strength. (Anisotropically consolidated undrained stress-controlled triaxial test at constant mean total stress with shear stress reversal; site: Amauligak I-54; borehole: 87 CRI ISI; sample depth: 46.0 m.)

pressive strength needs to be slightly greater (160 kPa versus 155 kPa) and σ_{ho} slightly lower (1670 kPa versus 1690 kPa) to get equivalent fit to the isotropic strength case, Fig. 7*a*.

The choice of $\beta = 1.3$ is motivated by a desire to explore an opposite trend to the obvious postulate. It can be seen from Fig. 8 that, again, only modest changes occur in interpretation of test data, and as expected these are in the opposite sense; the revised value of σ_{ho} under the hypothesis that $\beta = 1.3$ is approximately 1730 kPa.

The fact that a 30% change in the unloading strength should have such modest consequences in terms of interpreted values of σ_{ho} might seem surprising. However, inspection of [29] indicates why it is so. About half of the pressure–volume relationship during contraction is determined by the stress field at the end of the expansion stage. This component is invariant as a function of β. Hence, the effect of strength anistropy (β) is rather less than might be expected.

A question arises as to whether one particular value of β is preferable to another. Inspection of Figs. 7*a* and Fig. 8 suggests that equal fits have been obtained with each value (i.e., $\beta = 1.0$, 0.7, and 1.3). Therefore, it follows that the SBP data itself cannot be used to define β. Indeed, this is an example of the general principle that *in situ* tests cannot be used to define both the details of a constitutive model and the associated numerical parameters. Additional information on the general constitutive behaviour of the clay in question must be available from laboratory tests before the SBP can be properly interpreted.

The value of β was estimated by constant-P undrained triaxial tests, with the sense of shear stress being reversed once the sample had been brought to approximately peak compressive shear strength. Stress reversal continued until the sample had been brought to peak strength in the opposite sense. The total stress path imposed on the clay by this laboratory test procedure simulates conditions adjacent to the SBP, and an example of the clay behaviour measured is shown in Fig. 9. It can be seen that the ratio of strength in loading to unloading is about $\beta = 0.83$; the SBP data from Fig. 5 has been modelled using this estimate of β and is shown in Fig. 10. Comparison of Fig. 10 with 7*a* shows scarcely any improvement in fit and negligible change in inferred *in situ* parameters.

Discussion

Effect of disturbance during self-boring

One of the objections to inferring σ_{ho} from SBP data with the conventional methods is that the estimate of σ_{ho} may be significantly influenced by imperfect self-boring. The same question can be raised in the context of CAM of interpretation SBP data. The effect of imperfections in self-boring can be assessed by zero shifting existing test data.

An example of zero-shifted data is shown in Fig. 11. The data from Fig. 5 has been taken and the reference diameter corresponding to perfect self-boring arbitrarily shifted by more than 0.5% radial strain to mimic an SBP that has been advanced too fast into the ground during self-boring, so causing a radial displacement of the same amount. The fit of the model to the data is also shown in this figure. It can be seen that, although the fit has deteriorated, the constraining effect of the expansion and contraction limit pressures has served to keep the estimate of σ_{ho} sensibly constant compared with the "undisturbed" data. The reason for this can be appreciated by noting that the pressure–strain relationship is near horizontal at the limit pressures so that even large zero shifts have minimal effect on σ_{ho} when the model is constrained by both these limit pressures. Thus, the SBP can provide robust and reliable estimates of σ_{ho} even in the presence of finite amounts of disturbance. A good self-bored test does not have to be a perfect self-bored test, at least in the context of σ_{ho}.

Importance of the contraction data

The importance of contraction data to constrain the model for the SBP test is apparent from the above examples. However, the point can be reinforced by considering what happens if this constraint is not utilized.

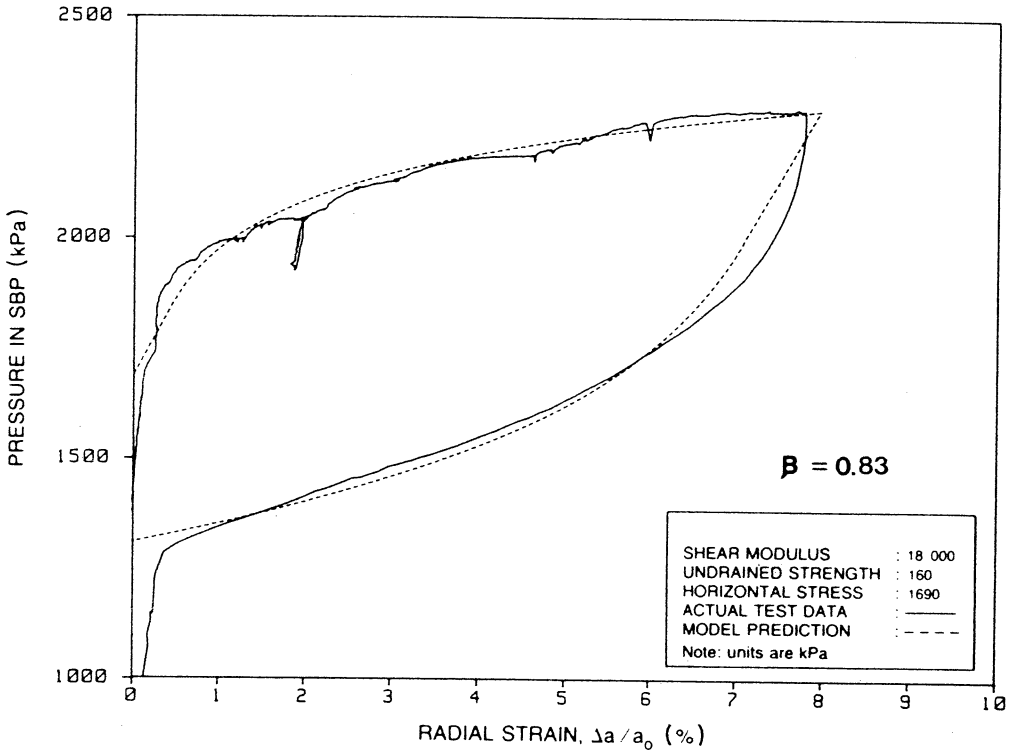

FIG. 10. Fit of model to data using β estimated from laboratory two-way triaxial test.

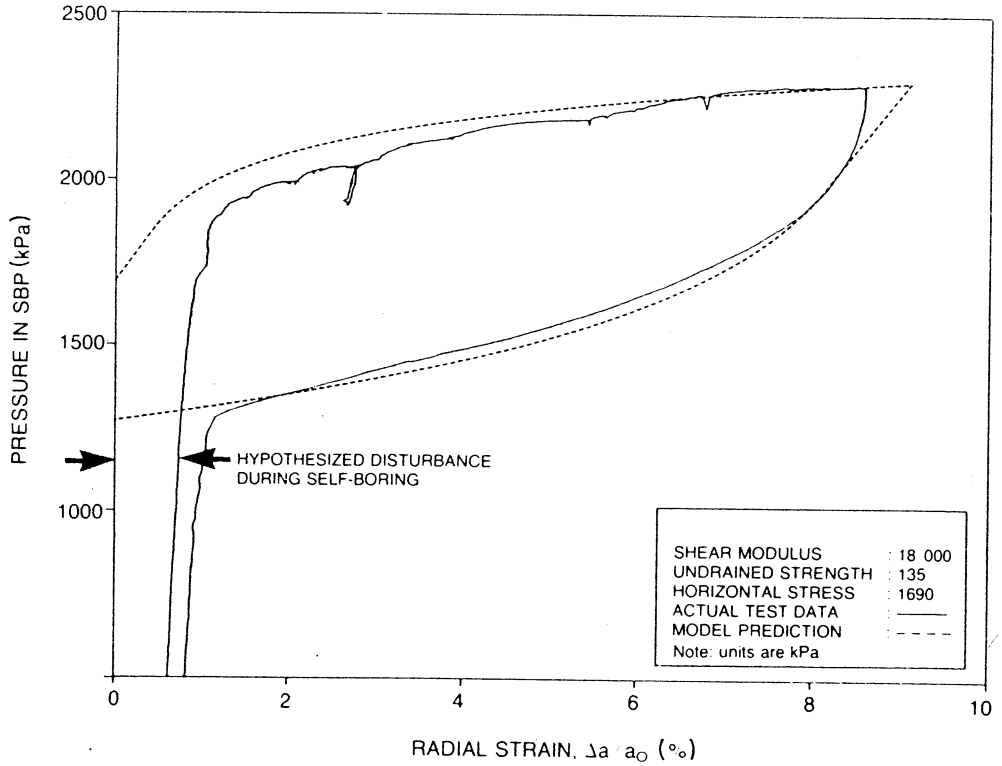

FIG. 11. Effect of disturbance during self-boring on estimate of σ_{ho}.

Computer-aided modelling of only the expansion phase of an SBP test amounts to an extended implementation of the graphical interpretation technique proposed by Marsland and Randolph (1977). Application to the previously discussed data is shown in Fig. 12*a*, from which it can be seen that it is possible to achieve a very much better fit of theory to test data than was achieved with the complete test (Fig. 7*a*) discussed before. It is particularly noteworthy that initial curvature, unload–reload modulus, and limit pressure are all well fitted.

Although Fig. 12*a* appears to be a satisfactory representation of the test data, this is not the case. Figure 12*b* shows the complete data set including the contraction phase with identical

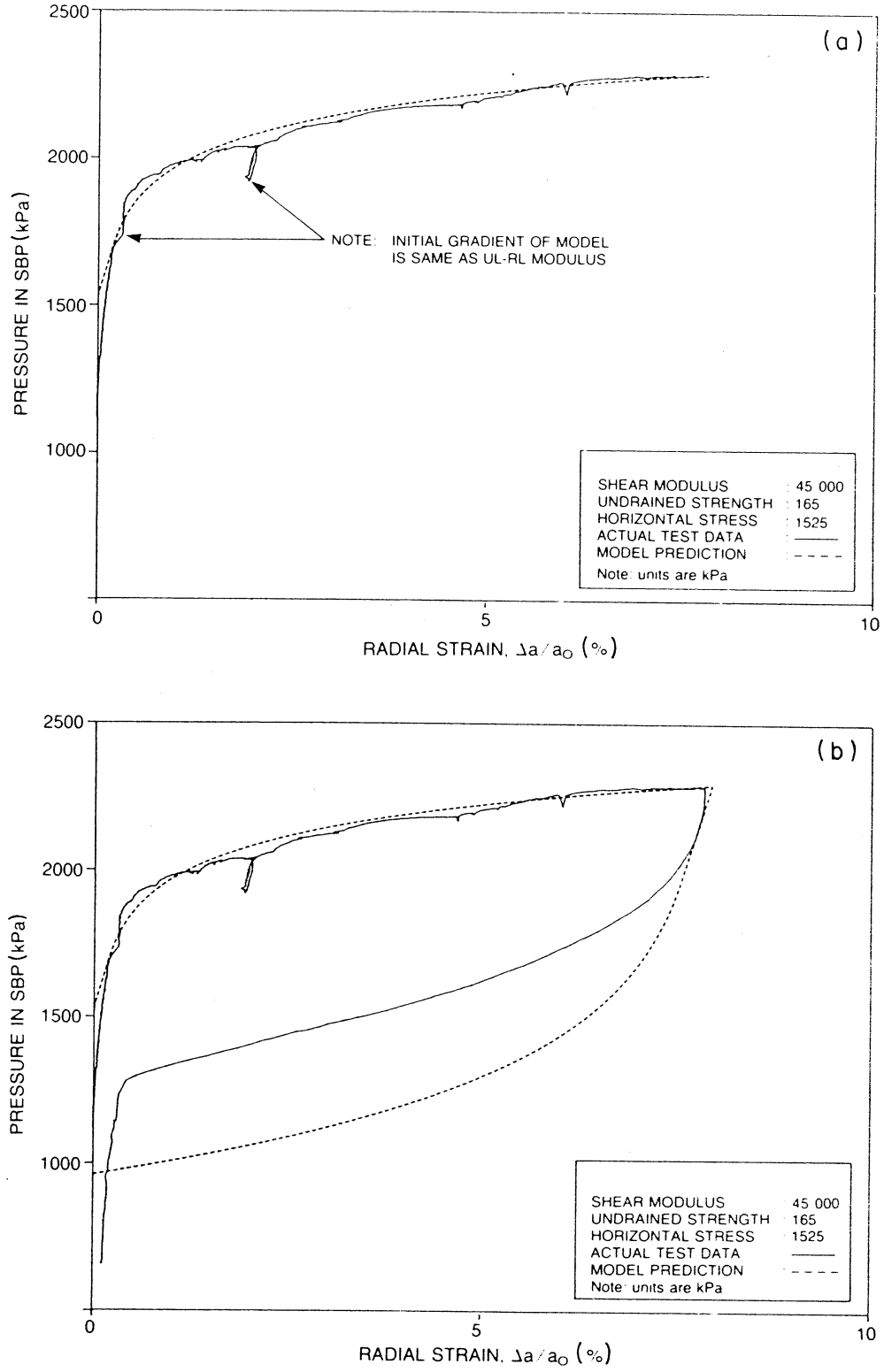

FIG. 12. Effect of considering expansion part only (*a*) rather than complete test (*b*).

model parameters to Fig. 12*a*. It is obvious that the strength has been substantially overestimated and, correspondingly, σ_{ho} underestimated.

The difference between Figs. 12*a* and 12*b* illustrates why it is so important to use a model for the complete pressuremeter test. There is simply a whole range of σ_{ho} and S_u values that will approximate an expansion curve; it is necessary to introduce a second data set—the contraction curve—to allow differentiation between the effect of σ_{ho} and the effect of S_u.

Relevance of strength anisotropy

Some effort was devoted to both measuring strength anisotropy and modelling its effect on interpretation of the SBP data. Although the effect of differing strengths in loading and

unloading is surprisingly small, the model does illustrate the general principal that there are limits to what may be achieved purely by *in situ* testing. As such it provides a clear caution to advocates of the sufficiency of *in situ* testing alone for site characterization. However, the consideration of strength anisotropy also provides evidence that the very simplest approach is sufficient for estimating horizontal geostatic stress. Further, comparison of the model with test data shown here makes it clear that the deficiency is not strength anisotropy but, rather, the inability to reconcile the actual elastic modulus of the ground with that required to model the test data, a direct consequence of using a simple elastic–plastic representation of clay.

Adequacy of the elastic–plastic model for clay

The model for the SBP test used in this paper is based on a simple elastic–plastic characterization of the clay. Examination of the triaxial test data shows this to be incorrect but that representation of work-hardening plasticity by a secant "elastic" modulus might be a reasonable approximation. And this is indeed found to be so when actual test data are modelled (Fig. 7*a*). The point to be appreciated is that one should not expect the value of "G" to correspond to the true elastic value as given by the unload–reload loop. Simultaneous matching of all parameters requires a more sophisticated model than a simple elastic–plastic representation. Thus, while the work presented here confirms the conclusion of Wroth (1984) that such a simple model is adequate for the interpretation of *in situ* test data, the caveat should be added that the elastic portion should not be treated as a true elastic modulus. In effect, true elasticity (energy storage) has been understated so that the effects of work hardening (increasing energy dissipation) may be modelled.

Conclusion

The Gibson–Anderson theory for pressuremeter interpretation has been extended to include the contraction phase for the particular case of self-bored pressuremeter testing. Interpretation of SBP data using this extended theory and the technique of computer-aided modelling provides robust and stable estimates of horizontal geostatic stress that are relatively unaffected by imperfect self-boring. The estimated value of σ_{ho} is not a function of the experience of the interpreter, provided due diligence is given to the task of fitting model to data. Once the model is fitted, the numerical values of the parameter are unarguable (at least within the validity of the assumptions in the theory).

Acknowledgements

Thanks are due to M. Hardy (Gulf), who provided a data processing shell with which to implement the model described here. The pressuremeter data were obtained by T. Jacklin and J. Graham (Thurber Consultants, Edmonton), while D. Horsefield and K. Been (Golder Associates, Calgary) carried out the laboratory testing of the clay. The thorough and detailed assessment of the paper by the two Journal reviewer's was also much appreciated.

ARNOLD, M. 1981. An empirical evaluation of pressuremeter test data. Canadian Geotechical Journal, **18**: 455–459

DENBY, G. M. 1978. Self-boring pressuremeter study of the San Francisco Bay mud. Ph.D. thesis, Department of Civil Engineering, Stanford University, Stanford, CA, Technical report CE-232.

GIBSON, R. E., and ANDERSON, W. F. 1961. *In-situ* measurement of soil properties with the pressuremeter. Civil Engineering and Public Works Review, **56**(658): 615–618.

HENDERSON, G., SMITH, P. D. K., and ST. JOHN, H. D. 1979. The development of a pressuremeter for offshore use. Proceedings, International Conference on Offshore Site Investigation, London, Paper 10.

HUGHES, J. M. O. 1973. An instrument for *in situ* measurement in soft clays. Ph.D. thesis, University of Cambridge, Cambridge, England.

HUGHES, J. M. O., and ROBERTSON, P. K. 1985. Full-displacement pressuremeter testing in sand. Canadian Geotechnical Journal, **22**: 298–307.

HUGHES, J. M. O., JEFFERIES, M. G., and MORRIS, D. L. 1984. Self-bored pressuremeter testing in Arctic offshore. Proceedings of 16th Offshore Technology Conference, Houston, OTC 4676.

JEFFERIES M. G., RUFFEL, J. P., CROOKS, J. H. A., and HUGHES, J. M. O. 1985. Some aspects of the behaviour of the Beaufort Sea clays. American Society for Testing and Materials, Special Technical Publication 883.

JEFFERIES, M. G., CROOKS, J. H. A., BECKER, D. E., and HILL, P. R. 1987. Independence of geostatic stress from overconsolidation in some Beaufort Sea clays. Canadian Geotechnical Journal, **24**: 342–356.

LACASSE, S., and LUNNE, T. 1982. *In-situ* horizontal stress from pressuremeter tests. Proceedings, Symposium on the Pressuremeter and Its Marine Applications, Éditions Techniq, Paris, France, pp. 187–208.

LACASSE, S., JAMIOLKOWSKI, M., LANCELLOTTA, R., and LUNNE, T. 1981. *In-situ* characteristics of two Norwegian clays. Proceedings, 10th International Conference on Soil Mechanics and Foundation Engineering, Stockholm, Vol. 2, pp. 507–511.

LAW, K. T., and EDEN, W. J. 1982. Effects of soil disturbance in pressuremeter tests. Updating Subsurface Sampling of Soils and Rocks and their *In-Situ* Testing, Engineering Foundation Conference, Santa Barbara, CA.

MARSLAND, A., and RANDOLPH, M. F. 1977. Comparisons of the results from pressuremeter tests and large *in-situ* plate tests in London clay. Géotechnique, **27**: 217–243.

MESRI, G., and CASTRO, A. 1987. C_α/C_c concept and K_0 during secondary compression. ASCE Journal of Geotechnical Engineering, **113**: 230–247.

WINDLE, D., and WROTH, C. P. 1977. *In-situ* measurement of the properties of stiff clays. Proceedings, 9th International Conference on Soil Mechanics and Foundation Engineering, Tokyo, Vol. 1, pp. 347–352.

WROTH, C. P. 1980. Cambridge *in-situ* probe. Symposium on Site Exploration in Soft Ground Using *In-situ* Techniques. United States Federal Highway Administration, FHWA-TS-80-202, pp. 97–135.

———1984. The interpretation of *in-situ* soil tests. The 24th Rankine Lecture. Géotechnique, **32**: 449–489.

List of symbols

- a radius of self-bored pressuremeter (= borehole radius); subscripted 0, 1, 2, 3, 4 to denote applicable stage of test, e.g., a_0 = radius of instrument in unpressurized condition
- p pressuremeter expansion pressure exerted on soil (i.e., after correction for membrane stiffness); also subscripted to denote test stage
- r radial coordinate
- θ circumferential coordinate
- r_{pe} radius of plastic–elastic interface during cavity expansion

r_{pc} radius of plastic–elastic interface during cavity collapse
σ stress; subscripts r = radial, θ = circumferential, a = axial
σ_{r_∞} far-field stress in horizontal plane, which may be alternatively called horizontal geostatic stress, σ_{ho}
S_u undrained shear strength of the clay
U_e excess pore-water pressure
G shear modulus of clay
β ratio of undrained strength of clay in extension to that in compression after principal stress reversal